



OPEN

A novel wavelength-adjusting method in InGaN-based light-emitting diodes

SUBJECT AREAS:

APPLIED PHYSICS

TWO-DIMENSIONAL MATERIALS

ELECTRONIC DEVICES

ELECTRONIC AND SPINTRONIC
DEVICESZhen Deng¹, Yang Jiang¹, Ziguang Ma¹, Wenxin Wang¹, Haiqiang Jia², Junming Zhou² & Hong Chen^{1,2}¹Key Laboratory for Renewable Energy, Beijing National Laboratory for Condensed Matter Physics, Institute of Physics, Chinese Academy of Sciences, Beijing 100190, China, ²Beijing Key Laboratory for New Energy Materials and Devices, Institute of Physics, Chinese Academy of Sciences, Beijing 100190, China.Received
19 August 2013Accepted
8 November 2013Published
17 December 2013Correspondence and
requests for materials
should be addressed to
H.C. (hchen@iphy.ac.
cn)

The pursuit of high internal quantum efficiency (IQE) for green emission spectral regime is referred as “green gap” challenge. Now researchers place their hope on the InGaN-based materials to develop high-brightness green light-emitting diodes. However, IQE drops fast when emission wavelength of InGaN LED increases by changing growth temperature or well thickness. In this paper, a new wavelength-adjusting method is proposed and the optical properties of LED are investigated. By additional process of indium pre-deposition before InGaN well layer growth, the indium distribution along growth direction becomes more uniform, which leads to the increase of average indium content in InGaN well layer and results in a redshift of peak-wavelength. We also find that the IQE of LED with indium pre-deposition increases with the wavelength redshift. Such dependence is opposite to the IQE-wavelength behavior in conventional InGaN LEDs. The relations among the IQE, wavelength and the indium pre-deposition process are discussed.

In recent years, both InGaN-based blue Light emitting diodes (LEDs) and AlGaInP LEDs have been developing rapidly and used widely in varies of applications^{1–7}. The AlGaInP material system is the primary material system for high brightness LEDs emitting in the long-wavelength part of the visible spectrum from 570 nm to 680 nm^{4–7}, while InGaN LEDs have been commercialized for short-wavelength applications below 530 nm^{1–3}. Neither InGaN nor AlGaInP LEDs can emit light efficiently in the range of 530 nm ~ 570 nm. The lack of high brightness LED in this region is known as “green gap”⁸. And light in this range is easiest to be sensed by human eyes, which gives it the advantages in many applications such as high luminous efficiency light source, full color display and noticeable indicator board.

For AlGaInP materials, there is an insurmountable barrier for pushing the emission wavelength down from red spectral regime to green spectral regime due to the energy band gap transferring from direct gap to indirect gap when the Al composition increases⁹. On the other hand, InGaN-based material system has attracted tremendous amount of attention over the past few years. The optical band gap of InGaN can be tuned from the near-ultraviolet to the near-infrared spectral range without indirect gap transformation, so it is possible to make LEDs at “green gap” using InGaN materials. The Internal quantum efficiency (IQE) of InGaN LED is quite high at blue regime but decreases rapidly when the wavelength increases after ~450 nm^{10–13}, which makes it difficult to realize high efficiency InGaN LEDs at “green gap” as long as such IQE-wavelength dependence exists.

In the conventional growth process, both changing the InGaN well thickness and indium content can adjust the wavelength^{10,14}. Since the LED efficiency is very sensitive to the InGaN well thickness, it is usually fixed at an optimum value of 2.5 nm in commercial LED products. Consequently reducing the growth temperature of InGaN quantum well layer is the main way to increase the wavelength by enhancing the indium corporation rate. Lower growth temperature leads to poor crystal quality and more impurities incorporated into InGaN well layer. Furthermore, when the indium content in the InGaN well layer increases, the polarization field will be enhanced^{15–21}, which makes the band bending more aggravated. These two factors both lower the IQE at higher indium content when longer wavelength demanded. Motivated by these considerations, new methods are needed to push the major emission peak towards longer wavelength without reducing the IQE.

Atoms pre-deposition method before a certain layer growth is commonly used in semiconductor material growth^{22–24}. In the Ge/Si or InGaAs/GaAs system grown by MBE, it has been demonstrated that the atoms pre-deposition can improve the atom content distribution. In this paper, we demonstrate a new way to adjust the emission wavelength without degrading IQE by indium pre-deposition in metal-organic chemical-vapor deposition technology.

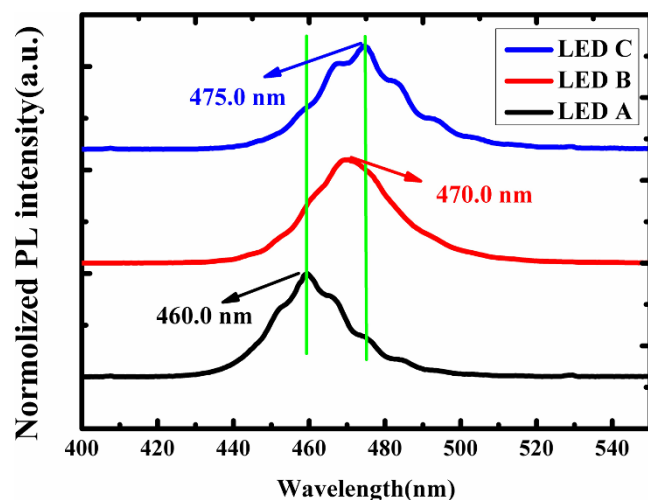


Figure 1 | The normalized PL spectra for all samples at room temperature (300 K). The major emission peak wavelengths for LED (A), (B), and (C) are 460.0, 470.0, 475.0 nm, respectively. The redshift value is about 15 nm.

Results

The normalized photoluminescence (PL) spectra are measured for all samples at room temperature (300 K). Figure 1 demonstrates that the major emission peak wavelengths for sample A, B, and C are 460.0, 470.0, 475.0 nm, respectively. According to the variation of peak wavelength, it is observed that the peak wavelength red-shifts with the increase of the indium pre-deposition time for LED A, B and C. This PL red-shift proved that the wavelength can be adjusted by the indium pre-deposition method.

High-resolution X-ray diffraction (HRXRD) measurements are carried out to study the relation between InGaN quantum well structure and indium pre-deposition process. Figure 2 shows (0002) plane reflection obtained by $\omega/2\theta$ scans along the growth direction for the three samples. The satellite peaks are clearly observed for all samples, indicating that the fine periodic multi-quantum wells (MQWs) structures are well formed. As shown in Fig. 2 (green line), compared to LED A, the InGaN diffraction peaks for LED B and C have a little shift outward the diffraction peak of GaN bulk material, which shows that the indium content varies slightly in the InGaN layer due to the indium pre-deposition, indicating that the pre-deposited indium is incorporated into InGaN/GaN MQWs. However, the spacing between the satellite peak positions, which determines the MQWs' period thickness, is exactly the same for these samples. The structure parameters obtained by the simulation fitting of the measured curves are presented in Table 1. The results present that the GaN barrier and InGaN well layers are all around 14 nm and 2.5 nm, respectively, indicating that the thickness is not affected by the pre-deposition. The average indium content of QWs increases along with the increase of the indium deposition time. The FWHM values of the InGaN “+1st” diffraction peak for the LED B and C are much smaller than that of LED A, which suggests that the uniformity of indium content distribution is improved due to the indium pre-deposition. It is also noted that the high series satellite peaks of

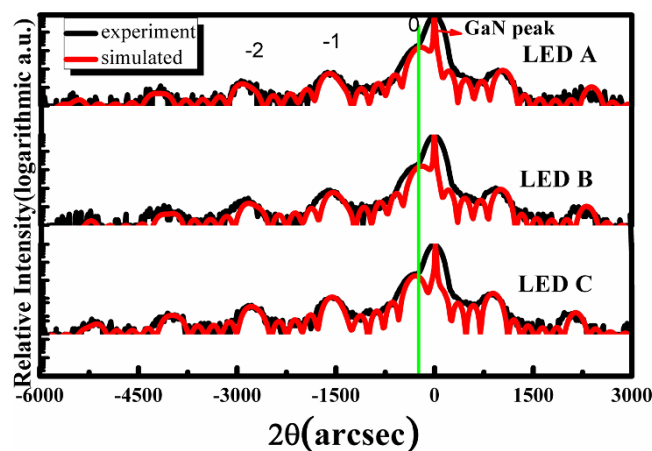


Figure 2 | HRXRD $\omega/2\theta$ scanning curves (black line) and simulations (red line) of LED A, LED B, and LED C. The green line shows that the InGaN diffraction peaks for LED B and C have a little shift outward the diffraction peak of GaN bulk material.

LED B, C is more distinct than that of LED A, which shows that the structure properties and the interface roughness between InGaN well layer and GaN barrier are significantly improved.

These changes in QW structure introduced by indium pre-deposition process are attributed to the indium segregation behavior, which causes indium content non-uniform distribution in InGaN wells^{25–28}. It is considered that Ga or In atoms exchange between the subsurface layer and the surface layer, and they tend to diffuse upward due to the lower energy states in the surface in the InGaN well layer growth process. But the diffusion is gradually weakened by the atoms accumulated in the surface layer until the exchange reaches dynamic balance. These theories have been demonstrated in Ge/Si²⁹ and InGaAs²² compound-semiconductor systems. In our experiment, the indium atoms accumulated in the surface layer by indium pre-deposition process prevent the atom diffusion from subsurface to surface layer in the following InGaN layer growth, which improves indium distribution uniformity and causes the average indium content increase, leading to the red-shift in the PL spectral.

The temperature-varied PL spectra for LED A, B and C are shown in Fig. 3 to compare their relative IQEs. The relative IQE is defined as the room temperature integrated PL intensity divided by the low temperature integrated PL intensity. Temperature dependence of normalized integrated PL intensity from LED A–C is shown in the Fig. 3, and their IQEs are 15.7%, 22.1% and 24.7%, respectively. The inset plot presents the dependence of IQE on the wavelength. Different from in conventional InGaN LEDs, the IQE become higher at longer emission wavelength with increase of indium deposition time.

In order to study the mechanism of unusual IQE-wavelength behavior in InGaN LEDs with indium pre-deposition, the integrated PL intensity V.S. temperature curve is analyzed using Arrhenius fitting. Nonradiative recombination centers (NRCs) exist in InGaN QWs and the activation energy of these NRCs is always smaller than the total QW binding energy of electrons and holes²⁸. Therefore, the luminescence thermal quenching of the InGaN LEDs is dominated

Table 1 | Structural parameters of InGaN/GaN MQWs of LED A, LED B, and LED C determined by HRXRD. (Chen)

Sample	Indium predeposition Time (min)	Period Thickness (nm)	Well thickness (nm)	Barrier thickness (nm)	Indium content of InGaN layer	FWHM of InGaN “+1st” diffraction peak
LED A	0	16.51	2.51	14	13.02%	267
LED B	1.5	16.50	2.50	14	13.52%	223
LED C	2	16.52	2.52	14	13.76%	201

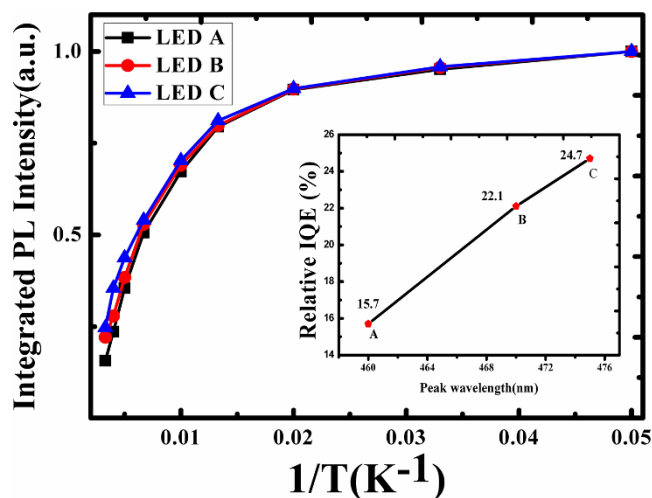


Figure 3 | Temperature dependence of normalized integrated PL intensity from LED A (solid square), LED B (solid circle), LED C (solid triangle). Inset: the IQE increase with the peak wavelength redshift and their IQEs are 15.7%, 22.1% and 24.7%, respectively.

by the nonradiative recombination process. If there are several kinds of NRCs, the integrated PL intensity can be fitted by the following expression^{30,31}:

$$I(T) \propto \frac{1}{1 + \sum_i S_i \exp\left(-E_i/k_B T\right)}$$

Where k_B is Boltzmann's constant, E_i are the activation energies of the corresponding NRCs, and S_i are factors related to the density of these centers. Two kinds of NRCs are considered here to obtain good fitting. The fitted parameters are shown in Table 2. LED A, B, and C have almost the same values of E_1 (~13 meV) and E_2 (~67 meV), respectively. This suggests that the same types of NRCs are shown in three samples. However, S_1 and S_2 of LED B and LED C are much smaller than those of LED A, which means that the number of effective NRCs is reduced by indium pre-deposition before the InGa_N well layer growth. Furthermore, it has been reported that in composition-nonuniform-distributed InGa_N layers due to segregation, the defect density near the InGa_N layer top is lower than that near the InGa_N layer bottom¹⁴. It is probably because the diffusion indium atoms from subsurface can leave sites for defect formation. This explains why S_1 and S_2 are smaller in LED B and LED C, where the indium atoms diffusion is suppressed by indium pre-deposition.

Discussion

In the light of the above, it is quite clear that the emission wavelength can be effectively adjusted by the indium pre-deposition method. It is noteworthy to mention here that the abnormal IQE-wavelength dependence observed in our experiment shows that the new method has competitive advantages over the conventional method in realizing high-efficiency long-wavelength InGa_N-based LEDs. However,

to push the emission wavelength of LEDs into “green gap” region, there are still lots of problems need to be solved. Compared to the blue InGa_N LEDs, the green InGa_N LEDs have higher indium content in MQWs, which requires lower growth temperature of InGa_N well layer. As a result, decomposition of NH_3 is insufficient and indium atoms are more difficult to incorporate into InGa_N well layer during MQW growth of green LEDs. Moreover, the higher indium content results in much stronger polarization field and indium phase separation is easier to occur. Therefore, more efforts are required to introduce the pre-deposition method to InGa_N-based green LEDs. For example, strain adjustment method may be combined with indium pre-deposition to solve the strain issues in green LEDs.

We have demonstrated the experimental realization of InGa_N/Ga_N MQWs LED with indium pre-deposition for adjusting the emission wavelength. The structure with indium pre-deposition shows higher average indium content and more uniform indium distribution than that of the conventional LED. An abnormal dependence of IQE-wavelength is observed from LEDs with different indium pre-deposition time. The IQE increases while the wavelength red shifts due to the decrease of defect density in the QWs. Furthermore, the results of HRXRD indicate that the high quality InGa_N well layer is obtained and the interface between InGa_N well layer and Ga_N barrier is improved. This finding may provide a train of thought to realize high efficiency LEDs emitting light in the “green gap” region.

Methods

The InGa_N/Ga_N MQW LED samples used in this study are grown on sapphire substrates by metal-organic chemical-vapor deposition. The precursors are trimethylgallium (TMGa), triethylgallium (TEGa), trimethylindium (TMIn), and ammonia (NH_3) respectively. The active region is grown on a 3 μm thick Si-doped Ga_N layer, followed by a 10 nm-GaN spacer layer and an 180 nm-thick Mg-doped Ga_N layer. For a comparative study, the LED A is a conventional one without indium pre-deposition. The InGa_N/Ga_N MQW active region consists of five 2.5-nm thick InGa_N well layers separated by 14-nm thick Ga_N barrier layers. Samples LED B and LED C are distinguished by adopting indium pre-deposition time. In LED B, C, prior to the growth of each InGa_N QW layer, indium atoms are deposited and the deposition time is 1.5 and 2 min, respectively. Then all the samples were characterized by HRXRD and temperature-dependent PL spectroscopy. HRXRD was performed using a Bede D1 double-axis diffractometer with a parabolic graded multilayer Gutman mirror collimator, followed by a four bounce channel-cut Si (2 2 0) monochromator, delivering a Cu $K\alpha_1$ line of wavelength $\lambda = 0.154056$ nm. Temperature-dependent PL spectra from 20 to 300 K were recorded using a 325 nm He-Cd continuous wave laser at an emission power. The emitted light was dispersed by a triple grating monochromator and detected by a GaAs photomultiplier tube using conventional lock-in technique.

1. Nakamura, S., Mukai, T. & Senoh, M. Candela-class high-brightness InGa_N/AlGa_N double-heterostructure blue-light-emitting diodes. *Appl. Phys. Lett.* **64**, 1687–1689 (1994).
2. Nakamura, S. The Roles of Structural Imperfections in InGa_N-Based Blue Light-Emitting Diodes and Laser Diodes. *Science*. **281**, 956–961 (1998).
3. Ponce, F. A. & Bour, D. P. Nitride-based semiconductors for blue and green light-emitting devices. *Nature*. **386**, 351–359 (1997).
4. Kuo, C. P. *et al.* High performance AlGaInP visible light emitting diodes. *Appl. Phys. Lett.* **57**, 2937–2929 (1990).
5. Kish, F. A. *et al.* Very high efficiency semiconductor wafer bonded transparent substrate ($\text{Al}_x\text{Ga}_{1-x}\text{In}_{0.5}\text{P}$ /GaP light emitting diodes. *Appl. Phys. Lett.* **64**, 2839–2841 (1994).
6. Gardner, N. F. *et al.* 1.4 \times efficiency improvement in transparent substrate ($\text{Al}_x\text{Ga}_{1-x}\text{In}_{0.5}\text{P}$ light-emitting diodes with thin (2000 Å) active regions. *Appl. Phys. Lett.* **74**, 2230–2232 (1999).
7. Krames, M. R. *et al.* High-power truncated-inverted-pyramid ($\text{Al}_x\text{Ga}_{1-x}\text{In}_{0.5}\text{P}$ /GaP light-emitting diodes exhibiting > 50% external quantum efficiency. *Appl. Phys. Lett.* **75**, 2365–2367 (1999).
8. KRAMES, M. R. *et al.* Status and future of high-power light-emitting diodes for solid-state lighting. *J. Display Technol.* **3**, 160–175 (2007).
9. Prins, A. D. *et al.* high pressure determination of AlGaInP band structure. *J. Phys. Chem. Solids*. **56**, 349–352 (1995).
10. Mukai, T., Yamada, M. & Nakamura, S. Characteristics of InGa_N-Based UV/Blue/Green/Amber/Red Light-Emitting Diodes. *Jpn. J. Appl. Phys.* **38**, 3976–3981 (1999).
11. Waltereit, P. *et al.* Nitride semiconductors free of electrostatic fields for efficient white light-emitting diodes. *Nature*. **406**, 865–867 (2000).

Table 2 | The fitted results with respect to the experimental results of temperature-dependent PL integrated intensities for LED A, LED B, LED C. (Chen)

Sample	S_1	$E_1(\text{meV})$	S_2	$E_2(\text{meV})$
LED A	2.41	13.63	105.96	67.82
LED B	2.31	13.07	34.29	66.45
LED C	1.57	12.58	24.62	67.63



12. Takeuchi, T. *et al.* Determination of piezoelectric fields in strained GaInN quantum wells using the quantum-confined Stark effect. *Appl. Phys. Lett.* **73**, 1691–1693 (1998).
13. Shapiro, N. A. *et al.* Luminescence energy and carrier lifetime in InGaN/GaN quantum wells as a function of applied biaxial strain. *J. Appl. Phys.* **94**, 4520–4529 (2003).
14. Li, Y. L., Huang, Y. R. & Lai, Y. H. Efficiency droop behaviors of InGaN/GaN multiple-quantum-well light-emitting diodes with varying quantum well thickness. *Appl. Phys. Lett.* **91**, 181113 (2007).
15. Park, S. H. & Chuang, S. L. Spontaneous polarization effects in wurtzite GaN/AlGaIn quantum wells and comparison with experiment. *Appl. Phys. Lett.* **76**, 1981–1983 (2000).
16. Park, S. H. & Chuang, S. L. Comparison of zinc-blende and wurtzite GaN semiconductors with spontaneous polarization and piezoelectric field effects. *J. Appl. Phys.* **87**, 353–364 (2000).
17. Park, S. H. & Chuang, S. L. Crystal-orientation effects on the piezoelectric field and electronic properties of strained wurtzite semiconductors. *Phys. Rev. B* **59**, 4725–4737 (1999).
18. Park, S. H. & Chuang, S. L. Crystal orientation dependence of many-body optical gain in wurtzite GaN/AlGaIn quantum-well lasers. *Semicond. Sci. Technol.* **17**, 686–691 (2002).
19. Takeuchi, T., Amano, H. & Akasaki, I. Theoretical study of orientation dependence of piezoelectric effects in wurtzite strained GaInN/GaN heterostructures and quantum wells. *Jpn. J. Appl. Phys.* **39**, 413–416 (2000).
20. Brown, I. H. *et al.* Time evolution of the screening of piezoelectric fields in InGaIn quantum wells. *IEEE J. Quantum Electron.* **42**, 1202–1208 (2006).
21. Vurgaftman, I. & Meyer, J. R. Band parameters for nitrogen-containing semiconductors. *J. Appl. Phys.* **94**, 3675–3696 (2003).
22. Kaspi, R. & Evans, K. R. Improved compositional abruptness at the InGaAs on GaAs interface by presaturation with In during molecularbeam epitaxy. *Appl. Phys. Lett.* **67**, 819–821 (1995).
23. Chattopadhyay, K. *et al.* Electroreflectance study of effects of indium segregation in molecular-beam-epitaxy-grown InGaAs/GaAs. *J. Appl. Phys.* **81**, 3601–3606 (1997).
24. Litvinov, D. *et al.* Transmission electron microscopy investigation of segregation and critical floating-layer content of indium for island formation in In_xGa_{1-x}As. *Phys. Rev. B* **74**, 165306 (2006).
25. Narukawa, Y., Kawakami, Y., Funato, M., Fujita, S. & Nakamura, S. Role of self-formed InGaIn quantum dots for exciton localization in the purple laser diode emitting at 420 nm. *Appl. Phys. Lett.* **70**, 981–983 (1997).
26. Tran, C. A. *et al.* Phase separation in InGaIn/GaN multiple quantum wells and its relation to brightness of blue and green LEDs. *J. Crystal. Growth*. **195**, 397–400 (1998).
27. Ramaiah, K. S. *et al.* Studies of InGaIn/GaN multiquantum-well green-light-emitting diodes grown by metalorganic chemical vapor deposition. *Appl. Phys. Lett.* **85**, 401–403 (2004).
28. Narukawa, Y., Kawakami, Y., Fujita, S. & Nakamura, S. Dimensionality of excitons in laser-diode structures composed of In_xGa_{1-x}N multiple quantum wells. *Phys. Rev. B* **59**, 10283 (1997).
29. Fukatsu, S., Fujita, K., Yaguchi, H., Shiraki, Y. & Ito, R. Selflimitation in the surface segregation of Ge atoms during Si molecular beam epitaxial growth. *Appl. Phys. Lett.* **59**, 2103–2105 (1991).
30. Bimberg, D., Sondergeld, M. & Grobe, E. Thermal Dissociation of Excitons Bounds to Neutral Acceptors in High-purity GaAs. *Phys. Rev. B* **4**, 3451–3455 (1971).
31. Hao, M., Zhang, J., Zhang, X. H. & Chua, S. Photoluminescence studies on InGaIn/GaN multiple quantum wells with different degree of localization. *Appl. Phys. Lett.* **81**, 5129–5131 (2002).

Acknowledgments

Supported by National High Technology Research and Development Program of China (grant nos. 2011AA03A112 and 2011AA03A106) and National Nature Science Foundation (grant nos. 11204360 and 61210014).

Author contributions

Hong Chen and Yang Jiang conceived and directed the research. Zhen Deng carried out all the samples growth experiments and fabricated the light emitting diodes. In the meanwhile, Zhen Deng carried out all the measurements including X-ray diffraction, temperature-varied photoluminescence. All the authors wrote the manuscript and discussed the results.

Additional information

Competing financial interests: The authors declare no competing financial interests.

How to cite this article: Deng, Z. *et al.* A novel wavelength-adjusting method in InGaIn-based light-emitting diodes. *Sci. Rep.* **3**, 3389; DOI:10.1038/srep03389 (2013).



This work is licensed under a Creative Commons Attribution-NonCommercial-ShareAlike 3.0 Unported license. To view a copy of this license, visit <http://creativecommons.org/licenses/by-nc-sa/3.0>



SUBJECT AREAS:

ELECTRONIC DEVICES

ELECTRONIC AND SPINTRONIC
DEVICES

APPLIED PHYSICS

TWO-DIMENSIONAL MATERIALS

SCIENTIFIC REPORTS:

3 : 3389

DOI: 10.1038/srep03389
(2013)

Published:

17 December 2013

Updated:

27 February 2014

CORRIGENDUM: A novel wavelength-adjusting method in InGaN-based light-emitting diodes

Zhen Deng¹, Yang Jiang¹, Ziguang Ma¹, Wenxin Wang¹, Haiqiang Jia², Junming Zhou² & Hong Chen^{1,2*}

¹Key Laboratory for Renewable Energy, Beijing National Laboratory for Condensed Matter Physics, Institute of Physics, Chinese Academy of Sciences, Beijing 100190, China, ²Beijing Key Laboratory for New Energy Materials and Devices, Institute of Physics, Chinese Academy of Sciences, Beijing 100190, China.

The details for affiliations 1 and 2 were incomplete in the original HTML and PDF versions of this Article. The affiliations were incorrectly listed as “¹Key Laboratory for Renewable Energy, Chinese Academy of Sciences, Beijing 100190, China” and “²Beijing Key Laboratory for New Energy Materials and Devices, Beijing 100190, China”. The correct affiliations are listed above. These have now been corrected in the HTML and PDF versions of the Article.